




Proceedings Article

Separating Nanoparticle Induced Delays from Relaxation Time Constant in TAURUS

Sevil Dilge Gulsun ^{a,b*}. Asli Alpman ^{a,b,c}. Emine Ulku Saritas ^{a,b}

^aDepartment of Electrical and Electronics Engineering, Bilkent University, Ankara, Turkey

^bNational Magnetic Resonance Research Center (UMRAM), Bilkent University, Ankara, Turkey

^cDepartment of Electrical Engineering and Computer Sciences, University of California Berkeley, CA, USA

*Corresponding author, email: dilge.gulsun@bilkent.edu.tr

© 2025 Gulsun *et al.*; licensee Infinite Science Publishing GmbH

This is an Open Access article distributed under the terms of the Creative Commons Attribution License (<http://creativecommons.org/licenses/by/4.0>), which permits unrestricted use, distribution, and reproduction in any medium, provided the original work is properly cited.

Abstract

Magnetic nanoparticles (MNPs) exhibit relaxation behavior, introducing a delay in their magnetization alignment. The TAURUS method enables simultaneous estimation of the signal delay and the effective relaxation time constant. In this study, we propose a method to separately estimate the MNP induced delay and the system induced delay. We then demonstrate that the MNP induced delay and the relaxation time constant estimated via TAURUS show different trends, implying that they may capture different aspects of the MNP response.

I. Introduction

Magnetic nanoparticles (MNPs) exhibit relaxation effects due to thermal fluctuation and viscous friction, which introduces a delay in their magnetization alignment process. This relaxation process is influenced by the MNP characteristics and their environment, and is typically modeled as a first-order Debye process [1].

Previously, we presented the TAURUS (TAU estimation via Recovery of Underlying mirror Symmetry) method, which offers a framework to directly estimate the relaxation time constant (τ) from the MNP signal [2–4]. Notably, during τ estimation, TAURUS also determines a time shift that accounts for both the system delay and the additional delay stemming from the relaxation response of the MNPs [2, 3]. In this work, we propose a method to separately determine the MNP induced delay and the system induced delay, while estimating τ . We demonstrate with magnetic particle spectrometer (MPS) experiments that the MNP induced delay is different than τ , and that it potentially captures different properties of the MNP response.

II. Methods and Materials

II.I. System Induced Delay Estimation

Due to direct feedthrough interference, the baseline signal from an empty-bore measurement is proportional to the time derivative of the drive field (DF). Assuming an imperfect decoupling of the drive and receive coils, the acquired baseline signal from an experimental MPS setup inherently incorporates the unknown system-induced delay, t_s . This delay can be determined using the cross-correlation of the baseline signal, $s_b(t)$, and the time derivative of the applied DF, $\dot{B}(t)$, as follows:

$$t_s = \operatorname{argmax}_{\Delta t} \int_{-\infty}^{\infty} s_b(t) \dot{B}(t - \Delta t) dt \quad (1)$$

Figure 1b shows an example case, where $t_s = 77 \mu\text{s}$ at 1 kHz and 15 mT DF settings on our MPS setup.

II.II. Relaxation Metrics

TAURUS models the signal as a convolution of the adiabatic signal, $s_{\text{adiab}}(t)$, with an exponential kernel with

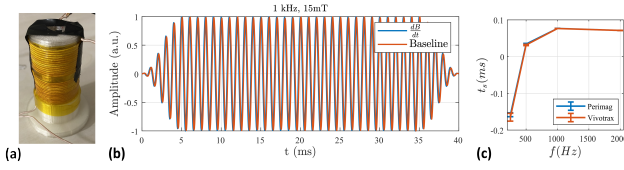


Figure 1: (a) Our in-house MPS setup. (b) An example baseline signal at 1 kHz and 15 mT DF settings, overlaid with the derivative of the applied DF. (c) The estimated system induced delays as a function of frequency for baseline signals acquired before Perimag and Vivotrax experiments.

time constant, τ [1, 3]:

$$s(t) = s_{\text{adiab}}(t) * r(t), \quad (2)$$

where

$$r(t) = \frac{1}{\tau} e^{-t/\tau} u(t). \quad (3)$$

Here, $u(t)$ is the Heaviside step function. Assuming that the received signal has mirror symmetry that has been broken due to relaxation, the relaxation time constant is computed as follows [2, 3]:

$$\tau(f) = \frac{S_{\text{pos}}^*(f) + S_{\text{neg}}(f)}{i2\pi f(S_{\text{pos}}^*(f) - S_{\text{neg}}(f))} \quad (4)$$

where $S_{\text{pos}}(f)$ and $S_{\text{neg}}(f)$ are the Fourier transforms of the positive and negative half-cycles of $s(t)$, respectively. While calculating τ , a time shift t_{edge} for which the signal best fits the model in (2) is also calculated. The correct (τ, t_{edge}) pair is estimated minimizing the following mean squared error [3]:

$$(\tau, t_{\text{edge}}) = \arg \min_{(\tau, t_{\text{edge}})} \int_0^{T/2} (\hat{s}_{\text{pos}}(t) - (-\hat{s}_{\text{neg}}(-t)))^2 dt \quad (5)$$

Here, T is the DF period, and $\hat{s}_{\text{pos}}(t)$ and $\hat{s}_{\text{neg}}(t)$ denote the positive and negative half-cycle signals after time shift compensation and deconvolution with the estimated relaxation kernel, which should restore mirror symmetry.

In this work, we assume that the time shift calculated by TAURUS directly reflects the sum of the system-induced delay, t_s , and the MNP induced delay, t_d :

$$t_{\text{edge}} = t_s + t_d. \quad (6)$$

Therefore, first τ and t_{edge} were estimated using the weighted least squares TAURUS method [4]. Then, the system induced delay computed via Eq. (1) was subtracted from t_{edge} to estimate t_d .

Finally, normalized versions of these metrics, $\hat{\tau}$ and \hat{t}_d , were computed by dividing with the DF period. These normalized metrics facilitate comparison of relative relaxation effects at different DF frequencies.

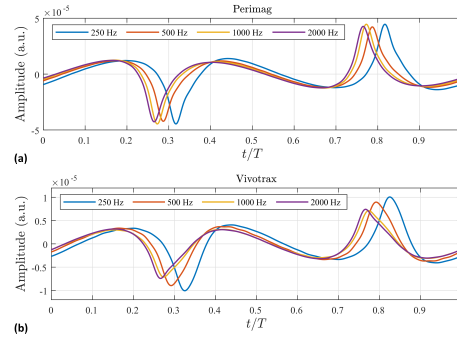


Figure 2: MPS signals for a) Perimag and b) Vivotrax, after compensating for system induced delays. The time axis is normalized by the DF period, and the signal amplitudes are normalized by the DF frequency to enable comparison.

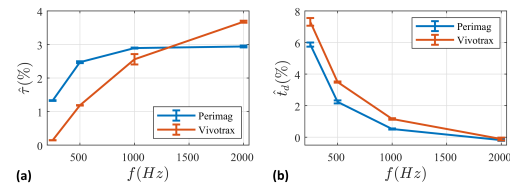


Figure 3: Relaxation metrics as a function of DF frequency for Perimag and Vivotrax MNPs. (a) $\hat{\tau}$ and (b) \hat{t}_d

II.III. MPS Experiments

The experiments were conducted on our in-house MPS setup, shown in Figure 1a. The measurements were taken at 15 mT DF amplitude at 4 different DF frequencies: 250 Hz, 500 Hz, 1 kHz, and 2 kHz. Two different MNPs were utilized: Perimag (Micromod GmbH, Germany) with 8.5 mg Fe/mL and Vivotrax (Magnetic Insight Inc., USA) with 5.5 mg Fe/mL, prepared at 125 μ L each. The experiments were repeated 2 times for each case.

III. Results and Discussion

Figure 1c shows that t_s at different DF frequencies remained consistent for Perimag and Vivotrax experiments, indicating that there was no noticeable system drift throughout the experiments. Here, the negative t_s values stem from delays in digital signal reception using a DAQ card. Figure 2 shows that the MPS signals demonstrate increased levels of asymmetric smearing at higher DF frequencies, but increased delay at lower DF frequencies. The relaxation metrics in Figure 3 show that, while the trends occur at different rates for Perimag and Vivotrax MNPs, $\hat{\tau}$ increases with DF frequency, whereas \hat{t}_d decreases with DF frequency. The fact that $\hat{\tau}$ and \hat{t}_d demonstrate opposite trends with respect to frequency implies that these two parameters may capture different aspects of the MNP response. For example, one of these two parameters may be more affected by Brown relaxation and

the other may be more affected by Neel relaxation.

As an alternative approach, the system delay t_s could also be estimated by measuring a transfer function, which would require additional measurements. In contrast, the proposed approach has the advantage of utilizing the baseline signal that is already measured right before MNP signal acquisition.

IV. Conclusion

This work shows that, after compensating for system induced delays, TAURUS estimates an MNP induced delay that may capture different aspects of the MNP response than the relaxation time constant. Jointly analyzing these two parameters may enable new color MPI techniques for applications such as viscosity mapping.

Acknowledgments

This work was supported by the Scientific and Technological Research Council of Turkey (TUBITAK

22AG016/23AG005 and 122E162).

Author's statement

Conflict of interest: Authors state no conflict of interest.

References

- [1] L. R. Croft, P. W. Goodwill, and S. M. Conolly. Relaxation in x-space magnetic particle imaging. *IEEE Transactions on Medical Imaging*, 31(12):2335–2342, 2012, doi:[10.1109/TMI.2012.2217979](https://doi.org/10.1109/TMI.2012.2217979).
- [2] M. Utkur, Y. Muslu, and E. U. Saritas. Relaxation-based viscosity mapping for magnetic particle imaging. *Physics in Medicine & Biology*, 62(9):3422, 2017, doi:[10.1088/1361-6560/62/9/3422](https://doi.org/10.1088/1361-6560/62/9/3422).
- [3] Y. Muslu, M. Utkur, O. B. Demirel, and E. U. Saritas. Calibration-free relaxation-based multi-color magnetic particle imaging. *IEEE Transactions on Medical Imaging*, 37(8):1920–1931, 2018, doi:[10.1109/TMI.2018.2818261](https://doi.org/10.1109/TMI.2018.2818261).
- [4] M. T. Arslan, A. A. Özaslan, S. Kurt, Y. Muslu, and E. U. Saritas. Rapid taurus for relaxation-based color magnetic particle imaging. *IEEE Transactions on Medical Imaging*, 41(12):3774–3786, 2022, doi:[10.1109/TMI.2022.3195694](https://doi.org/10.1109/TMI.2022.3195694).